ISSN: 0974-5823 Vol. 6 No. 3 December, 2021

International Journal of Mechanical Engineering

Physical Fields' Effect on Nonlocal Wave Propagation of Functionally Graded Nanotubes Based On Knudsen Flow Velocity

Mohammadreza Golriz[a] , Mir Abbas Roudbari[b]

[a]Environmental Research Institute, Academic Center for Education, Culture & Research (ACECR), Rasht, Iran

[b]Department of Mechanical Engineering, Langaroud Branch, Islamic Azad University, Langaroud, lran.

ABSTRACT

This study has analyzed the wave propagation of functionally-graded nanotubes surrounded by the Pasternak foundation using the Euler-Bernoulli beam model. A nanotube is affected by nanofluid flow and physical fields including thermal and magnetic fields. The support condition in different phases of the study was simple-simple. The kinematic equations were used based on Von Karman's theory. The flow equations were derived using Hamilton's rule. The Navier-Stokes (N-S) equations were used to express the fluid pressure. The magnetic field was extracted in 2-D mode from Lorentz relations. The effect of various parameters was analyzed on wave propagation of functionally graded nanotubes. The most underlying innovations in this study included analysis of wave propagation of functionally graded nanotubes under nanofluid flow in the Pasternak foundation and thermal and magnetic fields' effect on functionally graded nanotubes.

Key words: *Functionally Graded Nanotube, Wave Propagation, Pasternak Foundation, Physical Fields, Thermal and Magnetic Fields.*

INTRODUCTION

Nanostructures are available in all areas, whether in living or non-living things. Biologic nanostructures such as enzymes reveal that nature has created the best form of nanoscale technologies. Traditional sciences including physics, chemistry, mathematics, genetics, materials science, and biomedical engineering as independent activity domains in macro and micro scales tend to the unit principles, structures, and instruments on the nanoscale. Thus, nanotechnology sciences are deeply interdisciplinary and can provide tremendous achievements for human beings.

Nanofluids can be used for many purposes. Nanofluids have two uses including heat conveying and mass conveying. The majority of industrial uses of nanofluids are associated with cooling and heating as the subset of heat conveying. The nanofluids have medical and pharmacological uses in the field of mass conveying. Rashidi et al. [1] introduced a new model to analyze flowing nanofluid vibrations and studied the impact of the Knudsen number in this field. In this way, they used the Navier-Stokes (N-S) equations with modifying coefficients to analyze the nanofluids. Also, Ghavanloo [2] analyzed the vibrations and dynamic stability of fluid flow nanotubes using the Timoshenko-Ehrenfest beam theory and the Galerkin model. Zhang et al. investigated the wave propagation in nanotubes considering the surface effect [3]. Ghorbanpour and Rudbari studied the effect of initial and surficial stresses and Knudsen flow velocity in electric heat of nonlocal wave propagation of single-walled boron nitride nanotubes [4]. Ghorbanpour and Rudbari analyzed the effect of longitudinal magnetic field on wave propagation of single-walled carbon nanotubes using Knudsen number and surface considerations [5]. Simsek et al. analyzed the functionally graded nanobeams' bending and buckling based on Timoshenko's nonlocal Theory [6]. Nezamnejad et al. [7] studied the nonlocal nonlinear vibrations of functionally graded nanobeams. Barretta et al. investigated the equations of nonlocal functionally graded nanobeams based on the Euler-Bernoulli beam model [8]. The nonlocal thermal-mechanical vibrations of functionally graded nanobeams were analyzed by Ebrahimi and Salari [9]. Uymaz [10] studied the forced vibrations of functionally graded nanobeams using Eringen's model. Filiz and

Aydogdu analyzed the wave propagation of functionally graded nanotubes [11].

In the present study, wave propagation of functionally graded nanotubes surrounded by the Pasternak foundation was analyzed using the Euler-Bernoulli beam model. A nanotube is affected by nanofluid flow and physical fields including thermal and magnetic fields. The support condition in different phases of the study was simple-simple. The kinematic equations were used based on Von Karman's theory. The flow equations were derived using Hamilton's rule. The Navier-Stokes (N-S) equations were used to express the fluid pressure. The magnetic field was extracted in 2-D mode from Lorentz relations. The effect of different parameters was analyzed on the wave propagation of functionally graded nanotubes. The most underlying innovations in this study included analysis of wave propagation of functionally graded nanotubes under nanofluid flow in the Pasternak foundation and thermal and magnetic fields' effect on functionally graded nanotubes. The findings of this study can be used to design intelligent micro-proteins containing pharmaceutical liquid flowing in the living cell foundation to carry medicine and spray it on the desired area. Also, the micro-proteins are responsible for scanning the human organs in terms of measuring fat, cholesterol, blood sugar, and diagnosis of cancer cells, tumors, etc. Designing and constructing operators and sensors can be another use of the findings of this study.

Methodology

1. Flow equations

The flow equations are derived using the energy method, where total potential energy is defined as the summation of kinetic and strain energies, and the externally applied load works [12].

$$\Pi = K_T - U - W_{net} \quad (1)$$

Where; Π, K_T, U, and W_{net} respectively refer to total potential energy, kinetic energy, strain energy, and net externally applied workload.

2. Strain energy of functionally graded nanotubes

Strain energy for functionally graded nanotubes is given as [12]:

$$U = \frac{1}{2}\int_0^L \int_A^{\cdot} (\varepsilon_{xx}\sigma_{xx})\, dA\, dx \quad (2)$$

$$U = \frac{1}{2}\int_0^L \{\int_A^{\cdot} \sigma_x \left(-z\frac{\partial^2 w}{\partial x^2}\right) dA\} dx \quad (3)$$

Also [12-13]:

$$\int_A^{\cdot} \sigma_x\, z\, dA\, M_x = \quad (4)$$

Thus [11]:

$$U = \frac{1}{2}\{\int_0^L (D_{11}(\frac{\partial^2 w}{\partial x})^2)_{\}}\, dx \quad (5)$$

$$D_{11} = \int_{-\frac{d}{2}}^{\frac{d}{2}} (E_q d) dz \quad (6)$$

Where; refers to the diameter of functionally graded nanotubes.

3. Kinetic energy of functionally graded nanotubes

Kinetic energy for functionally graded nanotubes is defined as [11]:

$$K_T = \frac{1}{2}\{\int_0^L m_{11}(\frac{\partial w}{\partial x})^2\, dx + \rho_f A \int_0^L (\frac{\partial w}{\partial t})^2\, dx\} \quad (7)$$

$$m_{11} = \int_{-\frac{d}{2}}^{\frac{d}{2}} m_q\, dz \quad (8)$$

Where; w_i refers to the nanotube's lateral displacement, ρ_f refers to fluid mass density, and m_{11} refers to mass conveyed in functionally graded nanotubes. The changes in the properties of functionally graded nanotubes can be assumed in linear and exponential forms [11].

$$E_q^{\,linear}(z) = pz + s$$
$$m_q^{\,linear}(z) = pz + s$$
$$E_q^{\,Exp.}(z) = \beta_q e^{\delta_q z}$$
$$m_q^{\,Exp.}(z) = \beta_q e^{\delta_q z} \quad (9)$$

Where; q refers to the quality of upper and lower materials of functionally graded nanotubes.

4. Externally workload of functionally graded nanotubes

The load applied by the elastic foundation on functionally graded nanotubes assumed as the Pasternak model is defined as [13-14]:

$$F_{em} = K_w w - G_p \frac{\partial^2 w}{\partial x^2} \quad (10)$$

Where; K_w is Winkler's spring constant, and G_p is the shear modulus of the Pasternak model.

Magnetic fields are considered in the 2-D form in the whole study:

$$q = \chi \nabla \times \nabla \times (U \times H_x) \times H_x \quad (11)$$

Where; χ, U, and H_x respectively refer to magnetic permeability, displacement field, permanent magnetic field, and q refers to Lorentz force.

$$f_t = \int_{A_t} q dA_t + \frac{\partial}{\partial x}\int_{A_t} zq dA_t = \chi {H_x}^2 cos^2 \hat{\gamma} A_t \frac{\partial^2 w}{\partial x^2} - \chi {H_x}^2 sin^2 \hat{\gamma} I_t \frac{\partial^4 w}{\partial x^4} \quad (12)$$

Where; refers to magnetic field vector angle with the horizon.

The force caused by nanofluid conveying is defined as [16-17]:

$$F_{luid} = m_f \left(\frac{\partial^2 w}{\partial t^2} + 2 v_f \frac{\partial^2 w}{\partial x \partial t} + {v_f}^2 \frac{\partial^2 w}{\partial x^2}\right) + q\left(\frac{\partial^3 w}{\partial x^2 \partial t} + v_f \frac{\partial^3 w}{\partial x^3}\right) \quad (13)$$

Where; m_f is fluid mass, v_f is the internal fluid velocity, and q is fluid viscosity.

The fluid velocity of Knudsen number regarding the slip condition effects for nanofluid is defined as [18]:

$$V_{slip} = \left(\frac{1}{4\mu_0\left(\frac{1}{1+\hat{a}Kn}\right)}\right)\left(\frac{\partial P}{\partial x}\right)\left[{R_0}^2 - {R_i}^2 - 2{R_i}^2\left(\frac{2-\chi}{\chi}\right)\left(\frac{Kn}{1+Kn}\right)\right] \quad (14)$$

Where; Kn refers to the average dimensionless rate of the free path taken by fluid molecules with a certain length of fluid geometry. The value can be higher than a centesimal for the fluid conveying nanotubes. R_i and R_0 refer to internal and external nanotube radios, P refers to the fluid-induced pressure, and χ refers to the adaptive tangential torque coefficient equal to 0.7 [19].

$$\hat{a} = a_0 \frac{2}{\pi}\left[\tan^{-1}(a_1 Kn^B)\right] \quad (15)$$

Due to the value of experimental parameters including can give $a_0$0.04 , and = ,B, $a_1 = 4$ [19]:

$$\lim_{Kn \to \infty} \hat{a} = a_0 = \frac{64}{3\pi\left(1-\frac{4}{b}\right)} \quad (16)$$

Where; b is the total slip condition that is at (-1).

In no-slip mode, K_n is equal to $Kn = 0$. Thus, the correction coefficient of average velocity can be expressed as [20]:

$$VCF = \frac{V_{ave.slip}}{V_{ave.(no\ slip)}} = (1 + \hat{a}\, Kn)\left[1 + 4\left(\frac{2-\chi}{\chi}\right)\left(\frac{Kn}{1+Kn}\right)\right] \quad (17)$$

Hence, the equations can be obtained from the fluid-solid interaction. The $V_{ave.slip}$ must be replaced by $VCF \times V_{ave(no.slip)}$ in the equations. Effective viscosity of a fluid can be also obtained by [20]:

$$q^* = q\left(\frac{1}{1+\hat{a}\, Kn}\right) \quad (18)$$

Thus, let have [20]:

$$W_{net} = \frac{1}{2}\left[\int_0^l [-(K_w w - G_p \frac{\partial^2 w}{\partial x^2} + f_z A + F_{fluid})w - N_T \frac{\partial^2 w}{\partial x^2}] dx\right] \quad (19)$$

Where; refers to thermal force defined as [20]:

$$N_T = -\int_{-\frac{d}{2}}^{\frac{d}{2}} E_q \alpha_q (T - T_0)\, dz \quad (20)$$

Where; α_q and $\Delta T = T - T_0$ are thermal expansion coefficient and temperature variances respectively.

5. Hamilton's rule

The equations of lateral movements of functionally graded nanotubes are estimated using the principle of variances [20].

$$\int_{t_0}^{t_1} \delta\Pi\, dt = \delta \int_{t_0}^{t_1} (K_T - U - W_{net}) dt = 0 \quad (21)$$

Eq.21 is Hamilton's rule. Based on this rule, variances of strain energy, kinetic energy, and net externally applied workload are expressed as:

$$\delta U = \int_0^L D_{11} \delta\left(\left(\frac{\partial^2 w}{\partial x^2}\right)^2\right) dx \quad (22)$$

$$\delta K_T = \frac{1}{2}\left[\int_0^L m_{11} \frac{\partial w}{\partial t}\frac{\partial \delta w}{\partial t} + \int_0^L \rho_f A \frac{\partial w}{\partial t}\frac{\partial \delta w}{\partial t}\right] dx \quad (23)$$

$$\delta W_{net} = \int_0^L [\,(F_{em} + f_z + F_{fluid})\,\delta w + N_T \frac{\partial w}{\partial t}\frac{\partial \delta w}{\partial t}]\, dx \quad (24)$$

If using Hamilton's rule, δw is obtained as:

$$-\frac{\partial}{\partial x}\left(N_T\frac{\partial w}{\partial x}\right)+D_{11}\frac{\partial^2 w}{\partial x^2}+(m_{11}+\rho_f A)\frac{\partial^2 w}{\partial t^2}+F_{em}+f_z+F_{fluid}=0 \quad (25)$$

The boundary condition for simple-simple support is defined as [21]:

$$w(0.t)=\frac{\partial^2 w(0.t)}{\partial x^2}=0 \quad at \quad x=0 \quad w(L.t)=\frac{\partial^2 w(L.t)}{\partial x^2}=0 \quad at \quad x=L$$

(26)

6. Eringen's nonlocal theory

In the nonlocal continuous foundation mechanics model, stress on a point is assumed as a function of strain value in all areas of an object. Hence, the corrective theory contains information about the force between atoms, and the internal measure scale enters as the material's parameter in the structural equations. Eringen's nonlocal theory is the same microscale phenomenon. Eringen expressed the correlation between strain and stress for the homogeneous and isotropic elastic solids as [22]:

$$(1-(e_0 a)^2\nabla^2)\sigma = C : \varepsilon = \sigma^c \quad (27)$$

In the equation above, (:) shows the tensor coefficient, and C refers to the elastic stiffness tensor. σ is a nonlocal stress tensor, σ^c is a classic stress tensor, and ε is a strain tensor. e_0 is a constant specific to any material, and a is the material's internal length.

$$\mu = (e_0 a)^2 \quad (28)$$

Regarding the Eq.27, the equations of nonlocal anchors of functionally graded nanotubes can be defined as:

$$M_x - \mu M_x'' = -D_{11}\frac{\partial^2 w}{\partial x^2} \quad (29)$$

If replacing Eq.29 with Eq.25, let have:

$$[D_{11}+\mu G_p-\mu m_f(VCF)^2(V_{ave.(no\ slip)})^2+(\chi H_x{}^2\cos^2\hat{\gamma}A_t)\mu]w''''-[\chi H_x{}^2\sin^2\hat{\gamma}\,I_t\,\mu]w''''''-[\mu K_w+G_p+\chi H_x{}^2\cos^2\hat{\gamma}A_t+m_f(VCF)^2(V_{ave.(no\ slip)})^2]w''+\chi H_x{}^2\sin^2\hat{\gamma}\,I_t w''''+K_w w+\mu q^*[\dot{w}''''+(VCF)(V_{ave.(no\ slip)})w''''']-2\mu m_f(VCF)(V_{ave.(no\ slip)})\dot{w}''+2m_f(VCF)(V_{ave.(no\ slip)})\dot{w}'-q^*[\dot{w}''+(VCF)(V_{ave.(no\ slip)})w''']+(m_{11}+m_f)\ddot{w}-\mu(m_{11}+m_f)\ddot{w}''-(1-\mu\frac{\partial^2}{\partial x^2})(N_T)w''=0$$

(30)

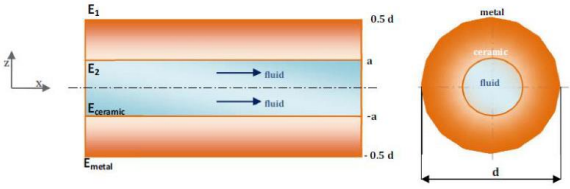

Figure 1. An element of functionally graded nanotube

To analyze the wave propagation in functionally graded nanotubes, a harmonic model is suggested to solve wave:

$$w(x.t) = \tilde{A}e^{i(kx-\omega t)} \quad (31)$$

Where; k , ω, and $\tilde{A}$ are respectively waves, circular frequency, and range. If replacing the equation in Eq.29, let have:

$$\vartheta_1\omega^2+\vartheta_2\omega+\vartheta_3=0 \quad (32)$$

Where;

$$\vartheta_1=(m_{11}+m_f)(1+\mu k^2)$$

$$\vartheta_2=i(qk^2+\mu qk^4)-2\mu m_f(VCF)(V_{ave.(no\ slip)})k^3-2m_f(VCF)(V_{ave.(no\ slip)})k^2$$

$$\vartheta_3=s_0k^6-s_1k^4+s_2k^2-i[q(VCF)(V_{ave.(no\ slip)})k^3+\mu q(VCF)(V_{ave.(no\ slip)})k^5]-$$

(33)

$$s_0=[\chi H_x{}^2\sin^2\hat{\gamma}\,I_t\,\mu]$$

$$s_1=[D_{11}+\mu G_p-\mu m_f(VCF)^2(V_{ave.(no\ slip)})^2+\mu N_T+\chi H_x{}^2\cos^2\hat{\gamma}A_t\mu+\chi H_x{}^2\sin^2\hat{\gamma}\,I_t]$$

$$s_2=[-G_p-\mu K_w+m_f(VCF)^2(V_{ave.(no\ slip)})^2-N_T-\chi H_x{}^2\cos^2\hat{\gamma}A_t]$$

(34)

The cut-off frequency is the frequency, at which the imaginary part becomes the number of the real wave. If placing $k=0$ in Eq.32, let have:

$$\omega_c=\sqrt{\frac{K_w}{m_{11}+m_f}} \quad (35)$$

Eq.32 is the solution to the desired project's problem, and the equation must be formulated in MATLAB to obtain appropriate diagrams.

In this study, the results are obtained in three modes including p=0, p=1, and p=2. If we have p=0, it means that there is an isotropic homogeneous beam. With P variances, E and ρ are obtained from the equations below.

$$E(x) = E_2 + (E_1 - E_2)V_f \quad (36)$$

$$\rho(x) = \rho_2 + (\rho_1 - \rho_2)V_f \quad (37)$$

$$V_f = (\frac{x}{L})^P \quad (38)$$

$$\frac{x}{L} = \frac{a}{d} \quad (39)$$

$$[a = 0.4\ (nm)\ \ d = 0.5\ (nm)]$$

$$E_r = \frac{E_2}{E_1} \quad (40)$$

$$M_r = \frac{\rho_2}{\rho_1} \quad (41)$$

In the equations above, V_f is volume fraction, is E_r, stiffness ratio, M_r is mass ratio, and P is a constant defines changes of materials' properties longitudinally.

Results

Using the equations of the methodology, and MATLAB encoding, frequency variance, and damping ratio diagrams are drawn due to various parameters.

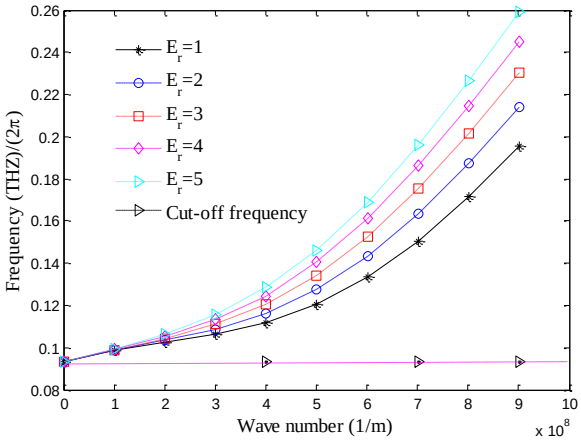

Figure 2. Wave frequency variance diagram due to wave number per different values of ceramic to metal stiffness ratio without surface effect

$T = 50(K).K_w = 10^9(N/m).H_x = 10^8(A/m).G_p = 10^{-9}(N/m).V_f = 10^3(m/s)$

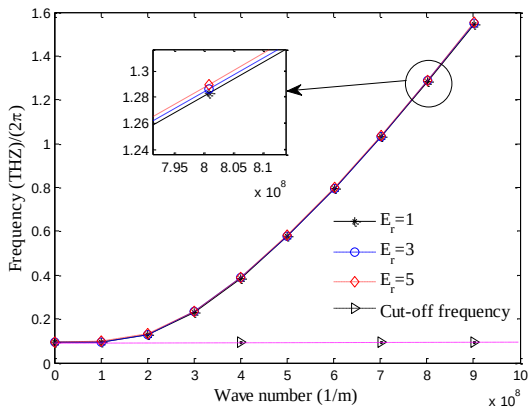

Figure 3. Wave frequency variances due to wave number per various values of ceramic to metal stiffness ratio with surface effect

$T = 50(K).K_w = 10^9(N/m).H_x = 10^8(A/m).G_p = 10^{-9}(N/m).V_f = 10^3(m/s)$

Figures 2 and 3 illustrate wave frequency variances per wave number per various values of stiffness ratio with and without surface effect. An increase in wave number increases the frequency in both modes. However, an increase in frequency with surface effect is more than it without surface effect. Also, frequency has been increased with the increase in stiffness ratio in both figures.

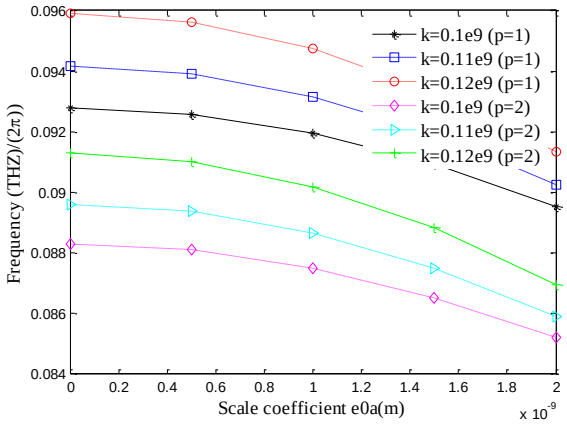

Figure 4. Frequency variances due to microscale parameters per various wavenumbers in p=1, p=2, $M_r = 2$, and E_r =2

$T = 50(K).K_w = 10^9(N/m).H_x = 10^8(A/m).G_p = 10^{-9}(N/m).V_f = 10^3(m/s)$

Figure 4 illustrates frequency variances due to microscale parameters per various wavenumbers in p=1 and p=2. The stiffness ratio and mass ratio in this figure are obtained at 2. Variances in wave number show that an increase in wave number

increases the frequency, and an increase in microscale parameter decreases the frequency. Also, the frequency in p=1 is more than p=2. This means that per linear volume fraction, higher frequency values can be obtained compared to exponential mode. Moreover, using size effects is important in the designation of nanotubes, and the classic model has a higher frequency than the nonlocal model.

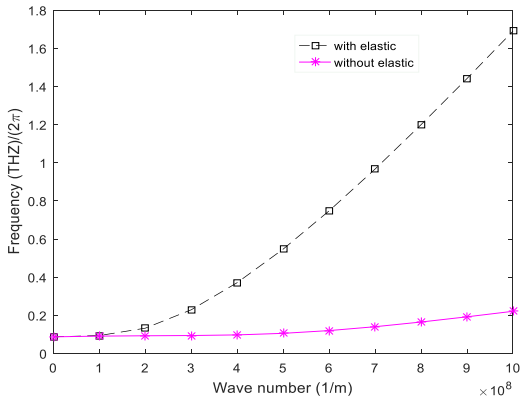

Figure 5. Frequency variances per wave number with and without elastic foundation in M_r=2 و E_r=2

$$T = 50(K).K_w = 10^9(N/m).H_x = 10^8(A/m).V_f = 10^3($$

Figure 5 illustrates the frequency variances per wave number with or without elastic foundation in p=1 and hardness and mass ratios. As the figure illustrates, the frequency is almost the same with and without elastic foundation in both cases. Then, the increase in frequency with elastic foundation is increased rapidly. Also, increased frequency without an elastic foundation is lower than it with an elastic foundation.

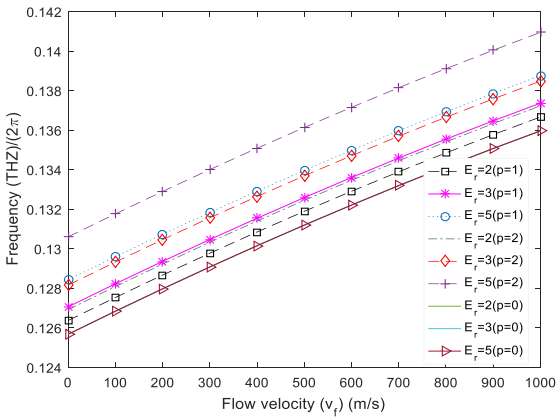

Figure 6. Frequency variances due to nanofluid flow velocity per various stiffness ratios for p=0, p=1, and p=2

$$T = 50(K).K_w = 10^9(N/m).H_x = 10^8(A/m).G_p = 10^{-9}(N/m)$$

Figure 6 illustrates frequency variances due to nanofluid velocity per various stiffness ratios for p=0, p=1, and p=2 modes. The mass ratio in this figure is equal to 1 and an increase in flow velocity can increase the frequency. Variances in stiffness ratio show that in stiffness ratios of 2, 3, and 5 in p=1 and p=2, an increase in stiffness ratio can increase the frequency. However, frequency is the same in p=0 per various stiffness ratios. The frequency is also decreased in p=1 and also p=2 modes.

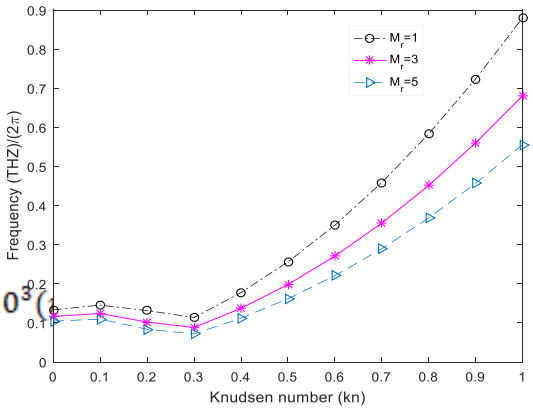

Figure 7. Frequency variances due to Knudsen number per various mass ratios

$$T = 50(K).K_w = 10^9(N/m).H_x = 10^8(A/m).G_p = 10^{-9}(N/m).V_f = 10^3(m/s)$$

Figure 7 illustrates frequency variances due to Knudsen number per various mass ratios. The stiffness ratio in this figure is equal to 1. Frequency is firstly decreased and then increased with an increase in the Knudsen number. Also, due to variances of mass ratio, it could be found that increased mass ratio can decrease the frequency. The initial variances can be due to flow velocity on walls.

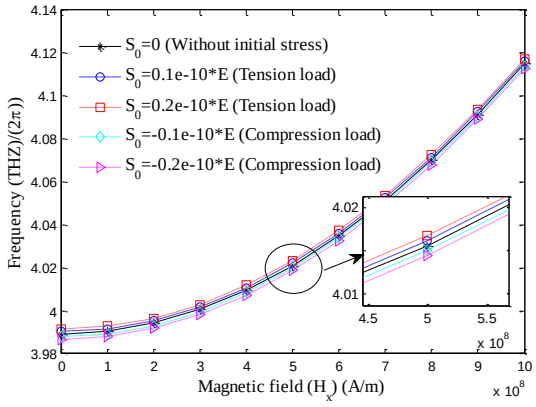

Figure 8. Frequency variances due to magnetic field intensity per various initial stress ratios in E_r=3 and M_r=3

$$T = 50(K).K_w = 10^9(N/m).G_p = 10^{-9}(N/m).V_f = 10^3(m/s)$$

Figure 8 illustrates the frequency variances due to magnetic field intensity per various initial stress ratios. The stiffness ratio and mass ratio are obtained at 3. An increase in magnetic field intensity increases the frequency, and an increase in initial stress increases the frequency.

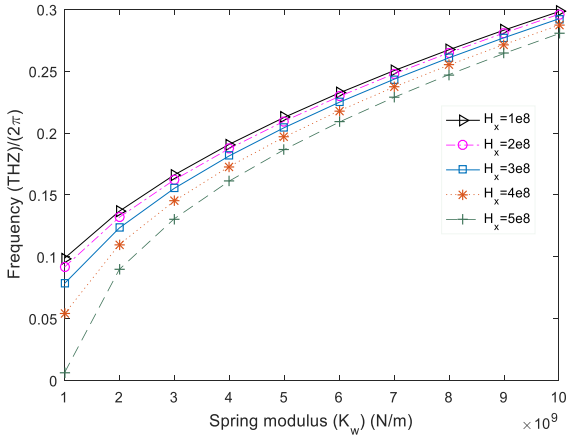

Figure 9. Frequency variances due to spring modulus (Winkler) per various magnetic field intensities

$$T = 50(K).G_p = 10^{-9}(N/m).V_f = 10^3(m/s)$$

Figure 9 illustrates the frequency variances due to spring modulus per various magnetic field intensities. The stiffness and mass ratios are equal to 1 in this figure. An increase in spring modulus increases the frequency, and an increase in magnetic field intensity decreases the frequency.

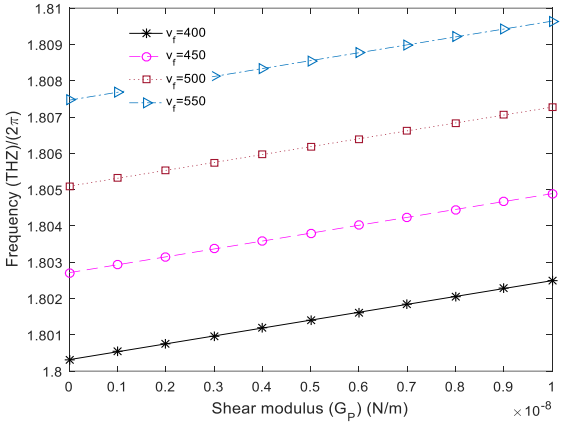

Figure 10. Frequency variances due to shear modulus per various flow velocities in E_r=3 and M_r=3

$$T = 50(K).K_w = 10^9(N/m).H_x = 10^8(A/m)$$

Figure 10 illustrates frequency variances due to shear modulus per various flow velocities. The stiffness and mass ratios are equal to 3 in this figure. An increase in shear modulus increases the frequency and an increase in flow velocity increases the frequency. The figures show that an increase in spring and shear modulus could increase wave frequency. The more the stiffness of the surrounding area of the functionally graded nanotube including spring and shear modulus becomes, the more the wave frequency increases.

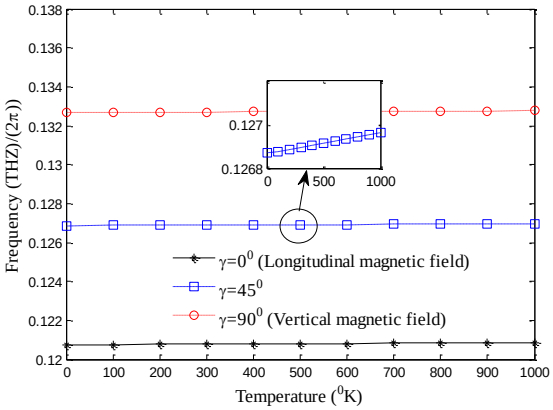

Figure 11. Frequency variances due to temperature from 0 to 1000°C per 0, 45, and 90° angles of the magnetic field with the horizon in E_r=2 and M_r=2

$$K_w = 10^9(N/m).H_x = 10^8(A/m).G_p = 10^{-9}(N/m).V_f = 10^3(m/s)$$

Figure 11 illustrates the frequency variances due to temperature per various magnetic field angles with the horizon. The stiffness and mass ratios in this field are equal to 2. With an increase in temperature,

the frequency remains almost unchanged; although it could be found that it is increased if looking more carefully. Also, an increase in horizontal magnetic field angle under fixed temperature could increase the frequency. In other words, the functionally graded nanotube modeling must be done under a horizontal magnetic field angle that is more stable than other modes.

The damping ratio is a dimensionless value in physics to show the way to analyze a fluctuating system and is shown with ζ. The damping ratio is the same imaginary part of frequency divided by the real part.

$$\zeta = -\frac{imag\ \omega}{real\ \omega} \qquad (41)$$

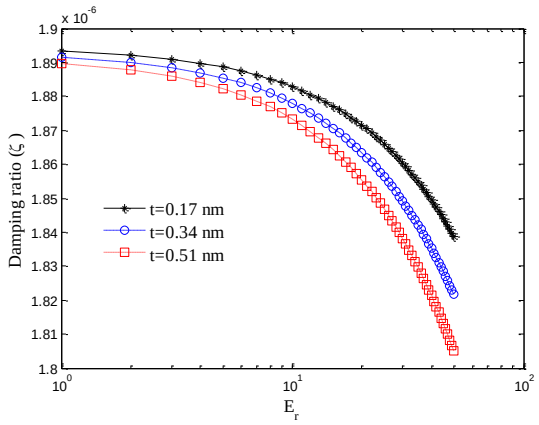

Figure 12. Damping ratio variances due to stiffness ratio per various nanotube thicknesses in $M_r = 3$

$T = 50(K).K_w = 10^9(N/m).H_x = 10^8(A/m).G_p = 10^{-9}(N/m).V_f = 10^3(m/s)$

Figure 12 illustrates the damping ratio variances due to the stiffness ratio per various nanotube thickness values. The mass ratio in this figure is given 3 and an increase in stiffness ratio decreases the damping ratio. Also, an increase in nanotube thickness decreases the damping ratio.

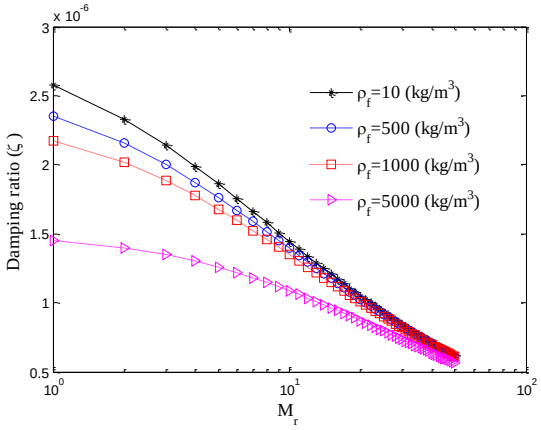

Figure 13. Damping ratio variances due to mass ratio per various flow mass densities in $E_r = 5$

$T = 50(K).K_w = 10^9(N/m).H_x = 10^8(A/m).G_p = 10^{-9}(N/m).V_f = 10^3(m/s)$

Figure 13 illustrates the damping ratio variances due to mass ratio per flow mass density. The stiffness ratio in this figure is given 5 and an increase in mass ratio decreases the damping ratio. Also, an increase in flow mass density decreases the damping ratio.

Table 1. Frequency variances due to microscale parameter variances

$k = 0.10 * 10^9(1/m)$	$P = 1$	$E_r = 2$	$M_r = 2$	$e_0a = 0(nm)$	$\omega =$ 0.0928 $(THZ/2\pi)$
				$e_0a = 0.5(nm)$	$\omega =$ 0.0926 $(THZ/2\pi)$
				$e_0a = 1(nm)$	$\omega =$ 0.0919 $(THZ/2\pi)$
				$e_0a = 1.5(nm)$	$\omega =$ 0.0909 $(THZ/2\pi)$
				$e_0a = 2(nm)$	$\omega =$ 0.0896 $(THZ/2\pi)$

Table 1 has presented the frequency variances due to the microscale parameter. The stiffness and mass ratio is equal to 2 in the table. The constant wave number shows that an increase in microscale parameter decreases the frequency.

Table 2. Frequency variances due to flow velocity variances

$P = 0$	$M_r = 1$	$E_r = 5$	$v_f = 100(m/s)$	$\omega = 0.127(THZ/2\pi)$
			$v_f = 300(m/s)$	$\omega = 0.129(THZ/2\pi)$
			$v_f = 500(m/s)$	$\omega = 0.1312(THZ/2\pi)$
			$v_f = 700(m/s)$	$\omega = 0.1332(THZ/2\pi)$
			$v_f = 900(m/s)$	$\omega = 0.135(THZ/2\pi)$
$P = 1$	$M_r = 1$	$E_r = 5$	$v_f = 100(m/s)$	$\omega = 0.1296(THZ/2\pi)$
			$v_f = 300(m/s)$	$\omega = 0.132(THZ/2\pi)$
			$v_f = 500(m/s)$	$\omega = 0.134(THZ/2\pi)$
			$v_f = 700(m/s)$	$\omega = 0.1358(THZ/2\pi)$
			$v_f = 900(m/s)$	$\omega = 0.1378(THZ/2\pi)$
$P = 2$	$M_r = 1$	$E_r = 5$	$v_f = 100(m/s)$	$\omega = 0.132(THZ/2\pi)$
			$v_f = 300(m/s)$	$\omega = 0.134(THZ/2\pi)$
			$v_f = 500(m/s)$	$\omega = 0.1362(THZ/2\pi)$
			$v_f = 700(m/s)$	$\omega = 0.1384(THZ/2\pi)$
			$v_f = 900(m/s)$	$\omega = 0.140(THZ/2\pi)$

Table 2 has presented the frequency variances due to flow velocity variances. The stiffness ratio is equal to 5 and the mass ratio is equal to 1 in the table. In various p modes, an increase in flow velocity has increased the frequency. The frequency in p=2 is higher than p=1, and p=0 shows the lowest frequency.

Conclusion

The results obtained from this study showed that the frequency was increased with and without surface effect, along with an increase in wavenumber. However, an increase in frequency with the surface effect is more than it without the surface effect, and the frequency is increased in this mode as a result of increased stiffness. An increase in microscale parameters increases the frequency. This shows that using the effects of size in the designation of nanotubes is an underlying factor. Also, the frequency in p=1 mode is more than p=2, and this means that the frequency per linear volume fraction mode is higher than in exponential mode. Also, the classic model showed a higher frequency than the nonlocal model.

With an increase in wavenumber, frequency increases with an elastic foundation more than it without an elastic foundation. An increase in flow velocity increases the frequency. In p=1 and p=2 modes, frequency increases with increased stiffness. In p=0 mode, frequency is the same per various stiffness values. The frequency is low in both p=1 and p=2 modes. An increase in Knudsen number causes decreased frequency at the first and increases it then. The initial variances are because of flow velocity on the walls. In this mode, frequency is decreased as a result of the increased mass ratio.

An increase in magnetic field intensity increases the frequency. The physical change in this incremental process is that the nanotube loses its balance with an

increase in magnetic field intensity, and faces a little turbulence. On the other hand, the nanotube tends to return to a balanced mode in the short term, and this makes a couple between the magnetic field and the nanotube's wave behavior, which increases the frequency. Also, an increase in initial stress increases the frequency. An increase in spring modulus increases the frequency, and the increased shear modulus increases the frequency too. The more the stiffness of the surrounding area of functionally graded nanotube including spring and shear modulus increases, the more the wave frequency would be increased.

An increase in temperature increases the frequency slightly, and an increase in horizontal magnetic field angle in fixed temperature increases the frequency. It would be better to take the model functionally graded nanotube under a magnetic field horizontally because it is more stable than other modes. An increase in stiffness ratio decreases the damping ratio, and an increase in flow mass density decreases the damping ratio too.

In this field, further studies must use visco-Pasternak's foundation to analyze the system wave propagation. Also, further studies must use other beam theories such as Riley, Timoshenko beam theory (TBT), and higher-order beam theory for further studies.

References

1. V. Rashidi, H.R. Mirdamadi, E. Shirani, A novel model for vibrations of nanotubes conveying nanoflow, Int. J. Comput. Mater. Sci. 51, 347–352 (2012).
2. E. Ghavanloo, F. Daneshmand, M. Rafiei, Vibration, and instability analysis of carbon nanotubes conveying fluid and resting on a linear viscoelastic Winkler foundation, Phys. E 42, 2218–2224 (2010).
3. YW. Zhang, TZ.Yang, J. Zang, B. Fang, Terahertz wave propagation in a nanotube conveying fluid taking into account surface effect. Mater Open Access, 6, 2393–9 (2013).
4. A. Ghorbanpour Arani, MA. Roudbari, Surface stress, initial stress, and Knudsen-dependent flow velocity effects on the electro-thermal nonlocal wave propagation of SWBNNTs, Physica B, Vol. 452, Pp. 159–165, (2014).
5. A. Ghorbanpour Arani, MA. Roudbari, Longitudinal magnetic field effect on wave propagation of fluid- conveyed SWCNT using Knudsen number and surface considerations., Applied mathematical modeling, Vol. 40, No.3, Pp. 2025–2038, (2016).
6. M. Simsek, HH. Yurtcu Analytical, solutions for bending and buckling of functionally graded nanobeams based on the nonlocal Timoshenko beam theory, Compos Struct 97, 378–86 (2013).
7. R. Nazemnezhad, S. Hosseini-Hashemi, Nonlocal nonlinear free vibration of functionally graded nanobeams, Compos Struct. 110, 192-199 (2014).
8. R. Barretta, L. Feo, R. Luciano, F. Moratti de Sciarra, Variational formulations for functionally graded nonlocal Bernoulli-Euler nanobeams. Compos Struct, 129, 80–9 (2015).
9. F. Ebrahimi, E. Salari, Nonlocal thermo-mechanical vibration analysis of functionally graded nanobeams in thermal environment, Acta Astronaut. 50, 113-129 (2015).
10. B. Uymaz, Forced vibration analysis of functionally graded beams using nonlocal elasticity, Compos Struct. 105, 227–239 (2013).
11. S. Filiz, M. Aydogdu, Wave propagation analysis of embedded (coupled) functionally graded nanotubes conveying fluid, Compos Struct. 132, 1260–1273 (2015).
12. S.A.M. Ghannadpour, B. Mohammadi, J. Fazilati, Bending, buckling and vibration problems of nonlocal Euler beams using Ritz method Composite Structures, Vol. 96, pp. 584-589 (2013).
13. J.N. Reddy, Nonlocal theories for bending, buckling, and vibration of beams, International Journal of Engineering Science, Vol. 45, pp. 288-307 (2007).
14. M.I. Friswell, S. Adhikari, Y. Lei, Int. J. Numer. Methods Eng. 71, 1365 (2007).
15. A. Ghorbanpour Arani, S. Amir, A.R. Shajari, M.R. Mozdianfard, Z. Khoddami Maraghi, M. Mohammadimehr, J. Mech. Eng. Sci. 224, 745 (2011).
16. N. Khosravian, H. Rafii-Tabar, J. Phys. D: Appl. Phys. 40, 7046 (2007).
17. L. Wang, Q. Ni, Mech. Res. Commun. 36, 833 (2009)
18. M. Mirramezani, H.R. Mirdamadi, Arch. Appl. Mech. s00419-011-0598-9 (2011).

19. G. Karniadakis, A. Beskok, N.Aluru: Microflows and Nanoflows: Fundamentals and Simulation. Springer, NY (2005)
20. Mehdi Mohammadi Mehr, Mohammad Salemi, Hossein Nasiri, Hassan Afshari, The effect of heat on the rise, critical buckling load and non-local Euler-Bernoulli beam vibrations on Pasternak elastic foundation using Ritz method, Modarres School of Mechanical Engineering, (2013).
21. P. Soltani, A. Farshidianfar, Periodic solution for nonlinear vibration of a fluid-conveying carbon nanotube, based on the nonlocal continuum theory by energy balance method applied Mathematical Modelling 36, 3712–3724 (2012).
22. Saleh Pourasmaili, Seyed Ahmad Fazelzadeh, The effect of precursor on the vibrations of viscoelastic bilayer nanosheets on the viscoelastic foundation, Modares School of Mechanical Engineering, Shiraz, (2015).